Photodissociation of Propionaldehyde at 248 nm: Roaming Pathway as an Increasingly Important Role in Large Aliphatic Aldehydes

ARTICLE *in* JOURNAL OF PHYSICAL CHEMISTRY LETTERS · DECEMBER 2013

Impact Factor: 7.46 · DOI: 10.1021/jz402329g

4 AUTHORS, INCLUDING:

Po-Yu Tsai
National Chung Hsing University
40 PUBLICATIONS **223** CITATIONS

SEE PROFILE

Hou-Kuan Li
National Taiwan University
4 PUBLICATIONS **19** CITATIONS

SEE PROFILE

THE JOURNAL OF PHYSICAL CHEMISTRY Letters

Letter

pubs.acs.org/JPCL

Photodissociation of Propionaldehyde at 248 nm: Roaming Pathway as an Increasingly Important Role in Large Aliphatic Aldehydes

Po-Yu Tsai, Kai-Chan Hung, Hou-Kuan Li, and King-Chuen Lin*

Department of Chemistry, National Taiwan University and Institute of Atomic and Molecular Sciences, Academia Sinica, Taipei 106, Taiwan

Supporting Information

ABSTRACT: Time-resolved Fourier transform infrared emission spectroscopy is employed in the photolysis of propionaldehyde (CH_3CH_2CHO) at 248 nm to characterize the role of the roaming pathway. High-resolution spectra of CO are analyzed to yield a single Boltzmann rotational distribution for each vibrational level ($\nu = 1-4$) with small rotational and large vibrational energy disposals. A roaming saddle point is found containing two far separated moieties of HCO and CH_3CH_2 with a weak interaction between them. Quasiclassical trajectory calculations on this configuration yield the CO energy flow behavior, consistent with the findings. The rate constant along the roaming pathway is evaluated to be larger by >1−2 orders of magnitude than those along tight transition state or three-body dissociation pathways. This work implies that the roaming mechanism plays an increasingly important role in aliphatic aldehydes as the molecular size becomes larger.

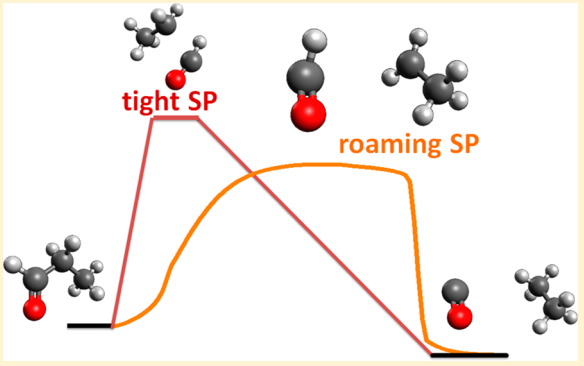

SECTION: Spectroscopy, Photochemistry, and Excited States

Aliphatic aldehydes are known to be present in the atmosphere through automobile exhaust or photooxidation of organic compounds.[1] Investigating their photodissociation mechanisms has been a main theme in photochemistry.[1−9] Upon UV irradiation, their excited states essentially lie in the $S_1(n,\pi^*)_{CO}$ band that undergoes internal conversion (IC) to the ground state S_0 from which molecular products, CO + alkane, are released. The S_1 state alternatively relaxes to triplet state T_1 via intersystem crossing (ISC) with which the radical channel, HCO + alkyl, is associated.

Among these aldehydes, formaldehyde (H_2CO)[2,10−14] and acetaldehyde (CH_3CHO)[4−9] were found to carry roaming signature in the photodissociation. Such a mechanism is essentially available in many molecular dissociations[11] and was first observed experimentally in formaldehyde by Moore and co-workers,[12] despite lack of detailed discussion. Like the tight transition state (TS) mechanism, there exists a first-order saddle point (SP) for the roaming process, as demonstrated in formaldehyde and acetaldehyde,[15,16] showing one small imaginary (harmonic) frequency along with some small-frequency modes. Two radical moieties in the roaming SP are weakly bound to each other such that they may have the chance to roam around varied configurations prior to the abstraction reaction. When the excitation energy increases, an alternative reaction channel of triple fragmentation (R + CO + H), resulting from a secondary decomposition of energized HCO, might open to interfere with the roaming pathway and thus hinder roaming identification.[17]

Propionaldehyde (CH_3CH_2CHO), as a member of aliphatic aldehydes, shows similar chemical properties as its smaller counterparts, but its photochemistry is much less investigated.[18−22] Kurosaki has demonstrated that CH_3CHO and CH_3CH_2CHO in photolysis at 248 nm may show dynamic similarity for their molecular production, $CH_3CHO \rightarrow CH_4 + CO$ and $C_2H_5CHO \rightarrow C_2H_6 + CO$.[23,24] Nevertheless, there is no experimental evidence to support such similarity in the energy flow between them. It is thus crucial to look into whether propionaldehyde is likely to exhibit a similar photodissociation feature. Herein, time-resolved Fourier transform infrared (FTIR) emission spectroscopy is employed to probe the HCO and CO fragments in propionaldehyde at 248 nm. The HCO temporal decay is monitored to inspect the efficiency of thermal decomposition, thereby identifying whether the triple fragmentation may occur. Internal energy disposal and rotational population distributions of the CO fragment are further analyzed with a previously adopted technique[6] to demonstrate the roaming signature, instead of the methods of ion imaging and laser-induced fluorescence.[2,4,5,25,26] Finally, the theoretical methods are performed in conjunction with the experimental findings to clarify dynamical complexity in photodissociation of propionaldehyde.

In the experiments with the step-scan FTIR emission spectroscopy,[27,28] the photolysis laser emitting at 248 nm

Received: October 29, 2013
Accepted: December 10, 2013
Published: December 10, 2013

propagated through the sample beam ejected at a pressure of ~0.5−1 Torr from an effusive nozzle that was housed in a reaction chamber. The fragment emission signals were guided to the entrance of the FTIR spectrometer in which the movable mirror of the interferometer was allowed to move step-by-step. The digitized signals were monitored and fed into a 200 kHz 16-bit transient digitizer for signal processing. The obtained interferograms were finally Fourier transformed to yield time-resolved spectra. The spectral responses of the beamsplitter, optical filters, and detection system were all calibrated using an IR emitter serving as blackbody-like radiation.

Upon irradiation of C_2H_5CHO at 248 nm in the presence of Ar at 3 Torr, a series of 5 μs resolved spectra of CO that appears at 1900−2200 cm^{-1} is well-resolved with a 0.25 cm^{-1} resolution up to J = 46, 45, 42, and 37 for ν = 1, 2, 3, and 4, respectively. (Figure S1 in the Supporting Information) The addition of Ar facilitates the IC efficiency with which the CO and C_2H_6 products are associated,and simultaneously quenches the rovibrational distributions of the resultant products if the delay time is long enough.[27,28]

Given the Einstein spontaneous emission coefficients, the population for each rotational line in the time-resolved spectra can be determined with the aid of spectral simulation. An example is given in Figure 1, showing comparison between

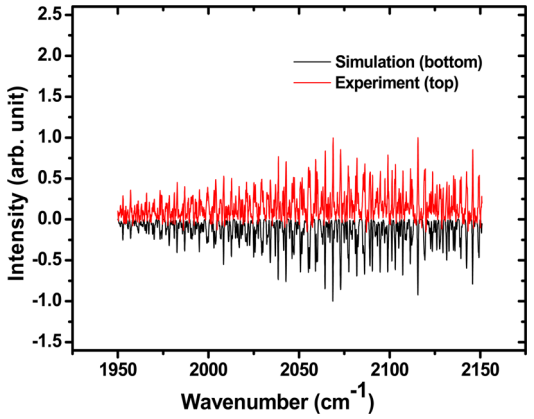

Figure 1. Comparison between the spectral simulation and observed spectrum of CO product.

simulation and the observed spectrum at 0 μs delay. As restricted to the instrument response time of 5 μs, the spectrum obtained at 0 μs delay is actually an average over the 0−5 μs duration. To achieve consistency between them, a fit with a single Boltzmann distribution of rotational population for each ν level is required. Accordingly, a semilogarithmic plot of $\ln[N_{\nu,J}/(2J+1)]$ versus $E_{\nu,J}$ for ν = 1−4 at 0 μs delay yields the Boltzmann rotational temperature from 870 to 1390 K (Figure S2 in the Supporting Information) that decreases to 300−400 K after the delay time is extended to 100 μs; $N_{\nu,J}$ is the relative population of CO in the (ν,J) level, and $E_{\nu,J}$ is the corresponding rotational energy. Note that the CO fragment may be rotationally relaxed to some extent even at 0 μs delay, whereas the vibrational to translational energy transfer is inefficient,[29] and thus, the CO vibrational population may well be considered as the nascent state. The rotational temperature as a function of the average delay time is then plotted and extrapolated to the real zero time (Figure S3 in the Supporting Information). Accordingly, the rotational temperature for CO ν = 1−4 is corrected to the range of 1450−940 K. Such a FTIR method is sensitive enough to distinguish different rotational population components with the aid of spectral simulation. For instance, with the same method, bimodal rotational distributions for methyl formate in ν = 1 and 2 are obtained, yielding branching ratios of roaming/tight TS pathways, which have been appropriately predicted by using quasiclassical trajectory (QCT) calculations on a reduced four-dimensional potential energy surface (PES).[30]

By summing up each rotational line at a given ν level, the time-dependent vibrational population is obtained, yielding vibrational population ratios of 0.49 ± 0.05, 0.28 ± 0.03, 0.15 ± 0.02, and 0.08 ± 0.01 for ν = 1, 2, 3, and 4, respectively, at 0 μs delay (Figure S4 in the Supporting Information). The rotational energy $E_{rot}(\nu)$ at a given ν may be evaluated by

$$E_{rot}(\nu) = \sum_{J=1}^{J=max} P_{\nu,J} E_{\nu,J} \quad (1)$$

where $P_{\nu,J}$ is the fraction of molecules populated at the J level. Given the above vibrational population ratio, the CO rotational energy disposal is averaged to be 2.1 ± 0.1 kcal/mol.[27,28] Further, the Boltzmann plot of $\ln(P_\nu)$ versus E_ν/k_B at 0 μs delay yields a straight line, from which the vibrational temperature is determined to be 5200 ± 100 K (Figure S5 in Supporting Information). Here, P_ν denotes the fraction of vibrational population, E_ν is the vibrational energy, and k_B is the Boltzmann constant. The population ratio for ν = 0, 1, 2, 3, and 4 at this vibrational temperature is estimated to be 0.47:0.26:0.14:0.08:0.05 with 10% uncertainty, and the vibrational energy yields 9.0 ± 0.6 kcal/mol with the zero-point energy included. Note that the CO fragment is obtained vibrationally hot and rotationally cold, in contrast to previous trajectory calculations yielding the rotational and vibrational energy of 18.0 and 5.2 kcal/mol, respectively.[23] The present work suggests that an alternative TS configuration should be required for the trajectory calculations.

Figure S6a in the Supporting Information shows a small profile of the HCO C−H stretch mode ν_1 at 2434.5 cm^{-1} and a large broad profile of C_2H_6 with double peaks of a CH_3 symmetric stretch ν_5 at 2896 cm^{-1} and a CH_3 asymmetric stretch ν_{10} at 2985 cm^{-1}. The HCO spectral intensity decays to vanish within 5−10 μs. The HCO relaxation time is consistent with that dissociated from acetaldehyde at 308 nm in which the reaction of triple fragmentation may not occur (Figure S6b (Supporting Information) and route 4 in Figure 2a). Thus, similarity of the temporal decay suggests that HCO from propionaldehyde at 248 nm should not decompose to any significant extent. When a large fraction of the HCO product is generated via the energized S_0 without encountering a potential barrier, the available energy tends to distribute to each fragment statistically. The C_2H_5 moiety with a large amount of vibrational degrees of freedom is allowed to gain a large internal energy. Thus, there is not enough internal energy left in HCO to undergo decomposition.

Figure 2 shows the dissociation pathways focusing on the related radical and molecular channels. The CO fragments are anticipated to result from the following routes (Figure 2a), (1) the energized S_0 state in the cis form (or (2) in the gauche form), which is dissociated directly to CO + CH_3CH_3 via a tight TS at 75.5 (83.7) (or 76.7 (85.1)) kcal/mol, and the same precursor undergoing three-body dissociation to (3) CH_2CH_2 + H_2 + CO via a TS at 68.4 (70.8) kcal/mol or (4) to C_2H_5 + H + CO. Similar pathways were also reported previously.[31] The

dx.doi.org/10.1021/jz402329g | J. Phys. Chem. Lett. 2014, 5, 190−195

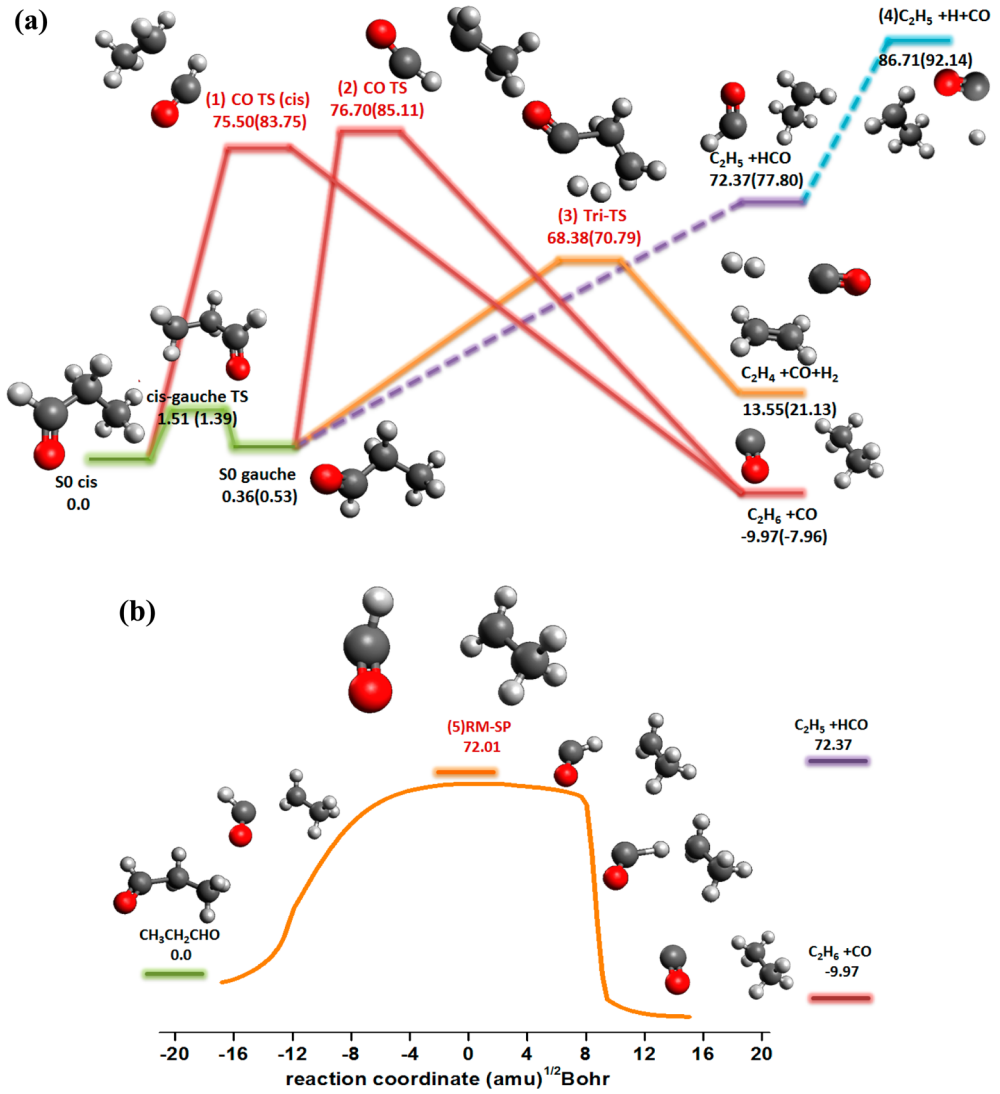

Figure 2. (a) Threshold energies (kcal/mol) and reaction pathways of radical and molecular channels on a C_2H_5CHO S_0 surface. (b) Roaming SPs and the intrinsic reaction coordinate (IRC). The formyl group proceeds in a flipping motion along the reaction path. Geometry optimizations were performed via CASSCF(6,6)/6-311++G(d,p). Energy values with and without parentheses were calculated by means of CCSD(T)/6-311++G(d,p) and CASSCF(10,9)/CASPT2/6-311++G(d,p), respectively. The IRC calculations in (b) were performed at the level of CASSCF(6,6)/6-31++G(d,p).

ethylene fragment owns a symmetric stretch mode ν_9 at 3105.5 cm^{-1} with a large Einstein spontaneous emission coefficient of 10.9 s^{-1} that is an average of 307 lines in the $\nu_9 = 1 \rightarrow 0$ transition from 3150 to 3170 cm^{-1}.[32] This coefficient is about twice smaller than 27.9 s^{-1}, an average in the $\nu_{10} = 1 \rightarrow 0$ transition of C_2H_6.[32] However, we cannot find any signal for this stable molecule in the 3150−3170 cm^{-1} region especially after a 10 μs delay (Figure S6, Supporting Information).

As with acetaldehyde and formaldehyde,[15,16] an additional roaming SP (route 5) has been found in propionaldehyde to have a similar feature of the vibrational modes (Figure 2b), showing a very small imaginary vibrational frequency along with some modes of small frequencies. Table S1 in the Supporting Information lists the harmonic vibrational modes for the four TS structures (routes 1, 2, 3, and 5) calculated herein for comparison. In the roaming SP (Figure 2b), the C(1)H_3C(2)-H_2 and C(3)HO moieties are almost parallel to each other at a large C(2)−C(3) distance of 3.93 Å. The H atom of CHO oscillates slowly between these two moieties. The H abstraction by CH_3CH_2 may thus result in a weak restoring force that is exerted to CO causing a small torque and subsequently a small rotational energy deposition. In contrast, for the tight TS structure (routes 1 and 2), CH_3CH_2 is at a short C−C distance of 2.17 (2.20 for cis) Å from CHO. The H abstraction results in large translational and rotational energies partitioning to C_2H_6 + CO.

To characterize the energy flow for the roaming and tight TS pathways, the QCT calculations were performed on the individual TS configuration (routes 1, 3, and 5) with zero excess energy. Under Born−Oppenheimer approximation, classical trajectories can be effectively computed on an electronic structure to avoid a complicated global PES construction. The required potential energy and its derivatives were calculated under the CASSCF(6e,6o)/6-31++g(d,p) level by integrating the classical equations of motion via a Hessian-based predictor−corrector algorithm.[33] Figure 3a−c shows comparison of the QCT results regarding vibrational amplitudes of CO and H_3CH_2C−H after H abstraction and

dx.doi.org/10.1021/jz402329g | J. Phys. Chem. Lett. 2014, 5, 190−195

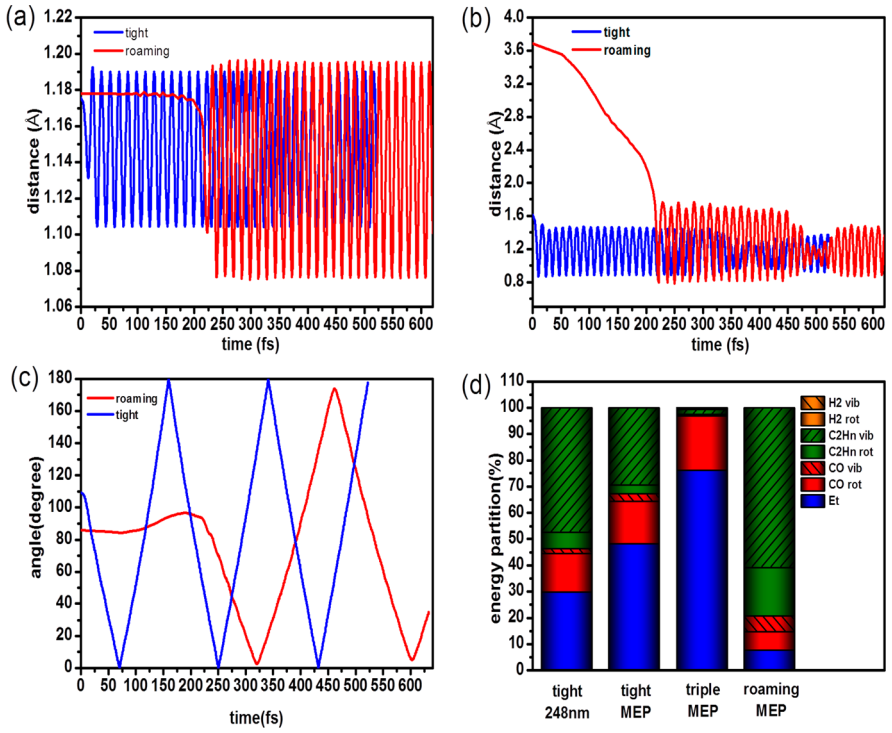

Figure 3. Time-dependent bond length/angle and energy disposals associated with ab initio molecular dynamics of roaming and tight CO (gauche form) SPs (routes 1 and 5). (a) The bond length variation of the CO product, (b) the C′−H′ distance variation of the $CH_3C'H_2H'$ product, and (c) the CO rotational angle variation with respect to the center-of-mass (c.m.) of the whole system along the dissociation coordinates of the above two mechanisms. Note that the rotational angle along the roaming pathway never reaches either 0 or 180°, indicating that the CO rotating plane and c.m.−C−O three-center plane are not coincident. In contrast, the CO rotation along the tight TS pathway is an in-plane motion. (d) Bar plots of relative energy disposals of propionaldehyde dissociation along different pathways. "Tight 248 nm" denotes QCT results on a tight TS configuration of C_2H_5CHO at 248 nm, adopted from ref 23. Tight MEP (route 1), triple MEP (route 3), and roaming MEP (route 5) indicate the QCT results on individual TS configurations along the minimum-energy path (MEP) or at zero excess energy.

the CO rotational period. The roaming molecular products apparently gain a larger CO and C_2H_6 vibrational energy but a smaller CO rotational energy. Note that in Figure 3c, the rotational angle along the roaming pathway never reaches either 0 or 180°, indicating that the CO rotating plane and c.m.−C−O three-center plane are not coincident. In contrast, the CO rotation along the tight TS pathway is an in-plane motion. This fact suggests that a pronounced $\nu-J$ vector correlation is found for the tight TS, but little or no $\nu-J$ correlation is found for the roaming. Such results are consistent with those $\nu-J$ correlation predictions for H_2CO and CH_3CHO by Bowmen and co-workers.[11] After analysis of the energy distribution (Figure 3d), as listed in Table S2 in the Supporting Information, CO via the roaming SP (tight TS) gains 17% (44%) available energy that is partitioned to the translational, vibrational, and rotational fractions of 4 (25), 6 (3), and 7 (16)%, respectively. Meanwhile, C_2H_6 obtains 83% (56%) available energy that is distributed to translation [3.8% (23.3%)], vibration [60.8% (29.4%)], and rotation [18.4% (3.3%)]. The roaming CO product tends to carry a small translational and rotational energy, whereas the C_2H_6 coproduct gains a large vibrational energy. In contrast, CO following the tight TS pathway gains a relatively large translational and rotational energy but small vibrational energy; the way of energy flow agrees with the prior QCT calculations performed at 248 nm.[23] Such a trend of energy distribution (Figure 3d) for roaming and tight TS mechanisms is essentially consistent with those reported previously.[2,4−14] The same QCT method was also performed on the three-body TS configuration ($C_2H_4 + H_2 + CO$), leading to a CO energy disposal in translational, vibrational, and rotational fractions of 39, 0.035, and 20%, respectively. The CO fragment via this mechanism gains an extremely small vibrational energy; again, the prediction is opposed to our observation.

This work was conducted under higher Ar pressure, instead of collision-free conditions. The CO product in C_2H_5CHO is obtained vibrationally hot, different from that in CH_3CHO obtained vibrationally cold. While inspecting the previous results of CH_3CHO,[7,8,34−36] the S_1/S_0 IC process seems to play a minor role (see the Supporting Information). Most fragments produced via the S_0 pathway are thus expected to follow a sequential ISC path, $S_1 \rightarrow S_1/T_1$ ISC $\rightarrow T_1 \rightarrow T_1/S_0$ ISC $\rightarrow S_0$. The molecular channel CO + CH_4, if generated along these ISC-based routes, retains a small available energy partitioning in the fragments such that the CO population may lie in low vibrational states. In C_2H_5CHO, the Ar collision-induced level-to-level coupling rate between S_1 and the dramatically increased density of states in S_0 at higher excitation energy like 248 nm may be enhanced more rapidly than S_1-T_1 coupling. Thus, a large available energy remains for the molecular channel, and CO may gain larger vibrational excitation energy.

Apart from the QCT calculations, the rate constants for each reaction channel may be further estimated. The roaming SP is lower by 3.49 (4.69) kcal/mol than the tight TS associated with the cis form (gauche form). According to a variational RRKM method,[37,38] Figure 4 shows that the roaming rate constant on the order of 10^{10} cm^3/molecule/s at 115.2 kcal/mol (or 248 nm) dominates over the pathways of tight TS and three-body

dx.doi.org/10.1021/jz402329g | J. Phys. Chem. Lett. 2014, 5, 190−195

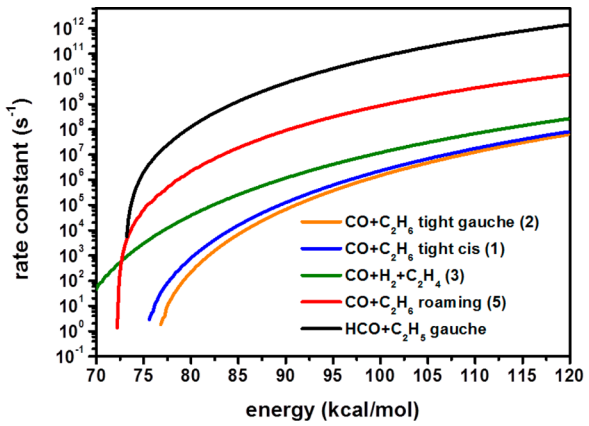

Figure 4. Energy dependence of microcanonical rate constants associated with five pathways, radical (dissociated from the gauche form), tight CO (gauche and cis forms), H_2 + CO + C_2H_4 (gauche form), and roaming pathway (cis form). The rate constants were evaluated by three methods, (1) VRC-TST (radical), (2) variational RRKM (roaming), and (3) RRKM (tight TSs).

dissociation. The rate constant for the radical channel is also accompanied, appearing larger than the roaming results. With the aid of QCT and RRKM evaluation, the roaming process is anticipated to dominate the products CO + C_2H_6 for propionaldehyde at 248 nm. All of the theoretical methods adopted are described in detail in the Supporting Information.

Note that the tight TS, roaming SP, and free radical pathways were treated dynamically independent herein. However, while comparing the cases of CH_3CHO and H_2CO, a steric effect of CH_3 in CH_3CHO may hinder abstraction of H from HCO, thereby slowing down the roaming reaction rate. Kable and coworkers thus defined a parameter *P* as a ratio of the roaming SP sum of states to the radical product sum of states that was determined to be 1 in H_2CO and 0.21 in CH_3CHO.[39] A smaller *P* is adjusted to reduce the roaming rate constant to fit the branching ratio of the roaming/radical pathway. The tight TS energy was lower by ∼5 kcal/mol than the roaming SP in H_2CO but became higher by <1 kcal/mol in CH_3CHO.[16] The corresponding branching ratios of the molecular product via the roaming/tight TS are 0.10/0.90 and 0.85/0.15 at 308 nm.[6,8,39] Despite steric hindrance in the roaming pathway, it is found that lowering the roaming SP, with respect to the tight TS, increases the important role of the roaming mechanism. In C_2H_5CHO, the roaming SP is stabilized by a larger C_2H_5 moiety appearing much lower in energy than the tight TS, thereby resulting in dominance of the CO + C_2H_6 products.

In conclusion, the roaming pathway in propionaldehyde serves as the minimum-energy route that is well below the conventional tight TS associated with the CO + C_2H_6 products. In view of kinetic and dynamic evidence, such a roaming mechanism is demonstrated to be the predominant route of the molecular channel. This work implies that the roaming pathway plays a general but increasingly important role in aliphatic aldehydes as the molecular size becomes larger. The findings of propionaldehyde roaming with two moieties of similar masses suggest that the concept of long-range reorientation is a more appropriate and an alternative description herein for the roaming signature.

■ ASSOCIATED CONTENT

Ⓢ Supporting Information

Six figures mentioned in the text, including time-resolved spectra of CO dissociated from propionaldehyde at 248 nm, CO fragment dissociated from propionaldehyde at 248 nm, a plot of the rotational temperature as a function of the average delay time, the time-dependent vibrational population of the CO fragment, a semilogarithmic plot of $\ln(P_v)$ of the CO fragment versus E_v/k_B at 0 μs delay, and the time-resolved infrared emission spectrum of HCO with the C−H stretch mode, a detailed description of vibrational energy disposal between C_2H_5CHO and CH_3CHO, and computation methods. This material is available free of charge via the Internet at http://pubs.acs.org.

■ AUTHOR INFORMATION

Corresponding Author

*E-mail: kclin@ntu.edu.tw. Fax: 886-2-23621483.

Funding

This work is supported by National Science Council of Taiwan, Republic of China under Contract No. NSC 99-2113-M-001-025-MY3.

Notes

The authors declare no competing financial interest.

■ REFERENCES

(1) Calvert, J. G.; Pitts, J. N., Jr., *Photochemistry*; John Wiley: New York, 1966.

(2) Townsend, D.; Lahankar, S. A.; Lee, S. K.; Chambreau, S. D.; Suits, A. G.; Zhang, X.; Rheinecker, J.; Harding, L. B.; Bowman, J. M. The Roaming Atom: Straying From the Reaction Path in Formaldehyde Decomposition. *Science* **2004**, *306*, 1158−1161.

(3) Cruse, H. A.; Softley, T. P. Velocity-Map Imaging Study of the Photodissociation of Acetaldehyde. *J. Chem. Phys.* **2005**, *122*, 124303.

(4) Houston, P. L.; Kable, S. H. Photodissociation of Acetaldehyde as a Second Example of the Roaming Mechanism. *Proc. Natl. Acad. Sci. U.S.A.* **2006**, *103*, 16079−16082.

(5) Rubio-Lago, L.; Amaral, G. A.; Arregui, A.; Izquierdo, J. G.; Wang, F.; Zaouris, D.; Kitsopoulos, T. N.; Banares, L. Slice Imaging of the Photodissociation of Acetaldehyde at 248 nm. Evidence of a Roaming Mechanism. *Phys. Chem. Chem. Phys.* **2007**, *9*, 6123−6127.

(6) Heazlewood, B. R.; Jordan, M. J. T.; Kable, S. H.; Selby, T. M.; Osborn, D. L.; Shepler, B. C.; Braams, B. J.; Bowman, J. M. Roaming is the Dominant Mechanism for Molecular Products in Acetaldehyde Photodissociation. *Proc. Natl. Acad. Sci. U.S.A.* **2008**, *105*, 12719−12724.

(7) Heazlewood, B. R.; Rowling, S. J.; Maccarone, A. T.; Jordan, M. J. T.; Kable, S. H. Photochemical Formation of HCO and CH_3 on the Ground S_0 ($1A'$) State of CH_3CHO. *J. Chem. Phys.* **2009**, *130*, 054310.

(8) Amaral, G. A.; Arregui, A.; Rubio-Lago, L.; Rodriguez, J. D.; Banares, L. Imaging the Radical Channel in Acetaldehyde Photodissociation: Competing Mechanisms at Energies Close to the Triplet Exit Barrier. *J. Chem. Phys.* **2010**, *133*, 064303.

(9) Rubio-Lago, L.; Amaral, G. A.; Arregui, A.; Gonzalez-Vazquez, J.; Banares, L. Imaging the Molecular Channel in Aacetaldehyde Photodissociation: Roaming and Transition State Mechanism. *Phys. Chem. Chem. Phys.* **2012**, *14*, 6067−6068.

(10) Suits, A. G. Roaming Atoms and Radicals: A New Mechanism in Molecular Dissociation. *Acc. Chem. Res.* **2008**, *41*, 873−881.

(11) Bowman, J. M.; Shepler, B. C. Roaming Radicals. *Annu. Rev. Phys. Chem.* **2011**, *62*, 531−553.

(12) van Zee, R. D.; Foltz, M. F.; Moore, C. B. Evidence for a Second Molecular Channel in the Fragmentation of Formaldehyde. *J. Chem. Phys.* **1993**, *99*, 1664−1673.

(13) Bowman, J. M.; Suits, A. G. Roaming Reactions: The Third Way. *Phys. Today* **2011**, *64*, 33−37.

(14) Yin, H. M.; Kable, S. H.; Zhang, X.; Bowman, J. M. Signatures of H_2CO Photodissociation from Two Electronic States. *Science* **2006**, *311*, 1443−1446.
(15) Shepler, B. C.; Han, Y.; Bowman, J. M. Are Roaming and Conventional Saddle Points for H_2CO and CH_3CHO Dissociation to Molecular Products Isolated from Each Other? *J. Phys. Chem. Lett.* **2012**, *2*, 834−838.
(16) Harding, L. B.; Klippenstein, S. J.; Jasper, A. W. Separability of Tight and Roaming Pathways to Molecular Decomposition. *J. Phys. Chem. A* **2012**, *116*, 6967−6982.
(17) de Wit, G.; Heazlewood, B. R.; Quinn, M. S.; Maccarone, A. T.; Nauta, K.; Reid, S. A.; Jordan, M. J. T.; Kable, S. H. Product State and Speed Distributions in Photochemical Triple Fragmentations. *Faraday Discuss.* **2012**, *157*, 227−241.
(18) Martinez, J. R. D.; Buitrago, A. A.; Howell, N. W.; Hearn, C. H.; Joens, J. A. The Near U.V. Absorption Spectra of Several Aliphatic Aldehydes and Ketones at 300 K. *Atmos. Environ., Part A* **1992**, *26*, 785−792.
(19) Terentis, A. C.; Knepp, P. T.; Kable, S. H. Nascent State Distribution of the HCO Photoproduct Arising from the 309 nm Photolysis of Propionaldehyde. *J. Phys. Chem.* **1995**, *99*, 12704−12710.
(20) Metha, G. F.; Terentis, A. C.; Kable, S. H. Near Threshold Photochemistry of Propanal. Barrier Height, Transition State Structure, and Product State Distributions for the HCO Channel. *J. Phys. Chem. A* **2002**, *106*, 5817−5827.
(21) Cordeiro, M. N. D. S.; Martinez-Nunez, E.; Fernández-Ramos, A.; Vázquez, S. A. Direct Dynamics Study of the Photodissociation of Triplet Propanal at Threshold. *Chem. Phys. Lett.* **2003**, *381*, 37−44.
(22) Buntine, M. A.; Lee, C.; Metha, G. F. The Lowest-Lying Excited Singlet and Triplet Electronic States of Propanal: An Ab Initio Molecular Orbital Investigation of the Potential Energy Surfaces. *Phys. Chem. Chem. Phys.* **2004**, *6*, 688−696.
(23) Kurosaki, Y. Energy-Flow Dynamics in the Molecular Channel of Propanal Photodissociation, $C_2H_5CHO \rightarrow C_2H_6 + CO$: Direct Ab Initio Molecular Dynamics Study. *J. Phys. Chem. A* **2006**, *110*, 11230−11236.
(24) Kurosaki, Y. Photodissociation of Acetaldehyde, $CH_3CHO \rightarrow CH_4 + CO$ II. Direct Ab Initio Molecular Dynamics Study. *Chem. Phys. Lett.* **2006**, *421*, 549−553.
(25) Chao, M.-H.; Tsai, P.-Y.; Lin, K.-C. Molecular Elimination of Methyl Formate in Photolysis at 234 nm: Roaming vs. Transition State-Type Mechanism. *Phys. Chem. Chem. Phys.* **2011**, *13*, 7154−7161.
(26) Grubb, M. P.; Warter, M. L.; Xiao, H.; Maeda, S.; Morokuma, K.; North, S. W. No Straight Path: Roaming in Both Ground- and Excited-State Photolytic Channels of $NO_3 \rightarrow NO + O_2$. *Science* **2012**, *335*, 1075−1078.
(27) Yeh, Y.-Y.; Chao, M.-H.; Tsai, P.-Y.; Chang, Y.-B.; Tsai, M.-T.; Lin, K.-C. Gas-Phase Photodissociation of CH_3COCN at 308 nm by Time-Resolved Fourier-Transform Infrared Emission Spectroscopy. *J. Chem. Phys.* **2012**, *136*, 044302.
(28) Hu, E.-L.; Tsai, P.-Y.; Fan, H.; Lin, K.-C. Photodissociation of Gaseous CH_3COSH at 248 nm by Time-Resolved Fourier-Transform Infrared Emission Spectroscopy: Observation of Three Dissociation Channels. *J. Chem. Phys.* **2013**, *138*, 014302.
(29) Tsai, P. Y.; Chao, M. H.; Kasai, T.; Lin, K. C.; Lombardi, A.; Palazzetti, F.; Aquilanti, V. Roads Leading to Roam. Role of Triple Fragmentation and of Conical Intersections in Photochemical Reactions: Experiments and Theory on Methyl Formate. *Phys. Chem. Chem. Phys.* **2013**, DOI: 10.1039/C3CP53792G, a paper that soon appears focuses on comparison of roaming branching for $\nu = 1$ and higher levels between FTIR and QCT results.
(30) Houston, P. L. *Chemical Kinetics and Reaction Dynamics*; Dover Publications, Inc.: Mineola, NY, 2001; pp 289−291.
(31) Chin, C.-H.; Lee, S.-H. Comparison of Two-Body and Three-Body Decomposition of Ethanedial, Propanal, Propenal, n-Butane, 1-Butene, and 1,3-Butadiene. *J. Chem. Phys.* **2012**, *136*, 024308.
(32) *The HITRAN database*. http://www.cfa.harvard.edu/hitran/ (2013).
(33) Millam, J. M.; Bakken, V.; Chen, W.; Hase, W. L.; Schlegel, H. B. Ab Initio Classical Trajectories on the Born−Oppenheimer Surface: Hessian-Based Integrators Using Fifth-Order Polynomial and Rational Function Fits. *J. Chem. Phys.* **1999**, *111*, 3800−3805.
(34) Heazlewood, B. R.; Maccarone, A. T.; Andrews, D. U.; Osborn, D. L.; Harding, L. B.; Klippenstein, S. J.; Jordan, M. J. T.; Kable, S. H. Near-Threshold H/D Exchange in CD_3CHO Photodissociation. *Nat. Chem.* **2011**, *3*, 443−448.
(35) Gherman, B. F.; Friesner, R. A.; Wong, T.-H.; Min, Z.; Bersohn, R. Photodissociation of Acetaldehyde: The CH_4 + CO Channel. *J. Chem. Phys.* **2001**, *114*, 6128−6133.
(36) Fu, B.; Han, Y.-C.; Bowman, J. M. Three-State Surface Hopping Calculations of Acetaldehyde Photodissociation to CH_3 + HCO on Ab Initio Potential Energy Surfaces. *Faraday Discuss.* **2012**, *157*, 27−39.
(37) Klippenstein, S. J.; Wagner, A. F.; Robertson, S. H.; Dunbar, R.; Wardlaw, D. M. *VariFlex Software*, version 1.0; Argonne National Laboratory, 1999.
(38) Zhu, L.; Hase, W. L. *RRKM*, a General RRKM program; Wayne State University, 1993.
(39) Andrews, D. U.; Kable, S. H.; Jordan, M. J. T.; Phase, A. Space Theory for Roaming Reactions. *J. Phys. Chem. A* **2013**, *117*, 7631−7642.